

Durham Research Online

Deposited in DRO:

15 March 2011

Version of attached file:

Published Version

Peer-review status of attached file:

Peer-reviewed

Citation for published item:

Platts, C.E. and Kaliteevski, M.A. and Brand, S. and Abram, R.A. and Iorsh, I.V. and Kavokin, A.V. (2009) 'Whispering-gallery exciton polaritons in submicron spheres.', *Physical Review B*, 79 (24). p. 245322.

Further information on publisher's website:

<http://dx.doi.org/10.1103/PhysRevB.79.245322>

Publisher's copyright statement:

© 2009 The American Physical Society

Additional information:

Use policy

The full-text may be used and/or reproduced, and given to third parties in any format or medium, without prior permission or charge, for personal research or study, educational, or not-for-profit purposes provided that:

- a full bibliographic reference is made to the original source
- a [link](#) is made to the metadata record in DRO
- the full-text is not changed in any way

The full-text must not be sold in any format or medium without the formal permission of the copyright holders.

Please consult the [full DRO policy](#) for further details.

Whispering-gallery exciton polaritons in submicron spheres

C. E. Platts, M. A. Kaliteevski, S. Brand, and R. A. Abram
Department of Physics, Durham University, DH1 3LE Durham, United Kingdom

I. V. Iorsh
Ioffe Institute, Polytechnicheskaya 26, 194021 St. Petersburg, Russia

A. V. Kavokin^{*}
Department of Physics, University of Rome II, 1 via della Ricerca Scientifica, Rome 00133, Italy
 (Received 17 November 2008; revised manuscript received 16 March 2009; published 23 June 2009)

We show that a semiconductor sphere with a radius comparable with the wavelength of light at the exciton resonance frequency can behave as a high-quality three-dimensional microcavity or “polariton dot.” We obtain numerical results for gallium arsenide submicron spheres and demonstrate that, in contrast to a larger sphere or planar microcavity, they can simultaneously possess both large quality factor and high finesse. In the strong-coupling regime the Rabi splitting approaches the bulk polariton splitting.

DOI: [10.1103/PhysRevB.79.245322](https://doi.org/10.1103/PhysRevB.79.245322)

PACS number(s): 71.36.+c

I. INTRODUCTION

Polariton lasers, theoretically proposed at the end of the 1990s, have recently been realized in various semiconductor structures, including planar microcavities and micropillars.^{1,2} Consequently, proposals for electrically pumped polariton lasers are a subject of much discussion in the literature.^{3–5} For the realization of room-temperature polariton lasers and the optimization of their characteristics several requirements need to be satisfied.⁶ First, the laser cavity should have a sufficiently high-quality (Q) factor in order to achieve the strong exciton-light coupling regime and a relatively long polariton radiative lifetime. Second, the finesse of the cavity should be high in order to eliminate the cavity photon modes close to the mode, which is strongly coupled with the exciton. Third, the density of polariton states should be reduced in order to facilitate the Bose-Einstein condensation (BEC) of exciton polaritons. The lower density of states results in a lower critical concentration of bosons needed to saturate all the excited states in the system and start populating the lowest energy state, i.e., the condensate.⁶ Fourth, the materials and the structure should be chosen so as to avoid the phonon bottleneck effect in exciton-polariton relaxation.⁶ As has been pointed out in recent reports,^{7–12} most of these criteria can be satisfied in certain structures that provide two-dimensional or three-dimensional photonic confinement and a polariton spectrum that is favorable for polariton energy relaxation and BEC. In particular, submicron semiconductor cylinders and spheres possess whispering-gallery modes with high Q factor and finesse and show real promise for polariton lasing applications.^{9,10} In contrast, supermicron cylinders and spheres have low finesse, which leads to exciton coupling with a number of modes simultaneously and a resultant complicated polariton spectrum with no ground state suitable for BEC.^{11,12} Despite the fact that the formalism describing the interaction of excitons with the photonic modes of a sphere is well developed, a complete and systematic analysis of the optical-mode spectrum is yet to be provided. In most of the literature on exciton polaritons in spheres, the only modes discussed have been those with the quantum number l , which

characterizes the relevant spherical harmonic equal to unity.^{11,13,14} [It is interesting to note that some works have also mistakenly considered the forbidden spherical modes with $l=0$ (Ref. 15)]. Further, the use of very rough estimates of the radiative decay of the photonic modes has not allowed the prediction of reliable criteria for the weak-strong-coupling threshold in spherical structures.¹²

The present theoretical work investigates submicron spheres, and particularly those made of gallium arsenide, for applications in polariton lasers. We systematically study the lifetime of the exciton-polariton modes in the cavity as a function of their quantum numbers and the radius of the sphere. By solving the Maxwell equations, while including the resonant exciton contribution to the dielectric response, we find the parameters of the system for which cavity modes with both high Q factor and high finesse exist in the spheres. Further, we show that the modes can exhibit anticrossings with the excitonic state characterized by a vacuum field Rabi splitting exceeding that of typical planar microcavities. We recognize that the interaction of light in systems of spherical symmetry with various excitations, for example, optical phonons¹⁶ and plasmons¹⁷ has been a subject of numerous studies, but the potential for analogy with other cases is limited. The present work also has a very distinctive applications oriented focus.

II. FORMALISM

A spherical electromagnetic wave can be described in terms of two independent types of mode, which are conventionally referred to as TE and TM.^{18,19} For a TE mode with frequency ω in a nonmagnetic medium with dielectric constant $\epsilon=n^2$ the fields are^{7,8}

$$\vec{E}_{l,m} = -\frac{k}{\sqrt{\epsilon}} \left(\frac{m}{\sin \theta} P_l^m(\cos \theta) \vec{e}_\theta + i \frac{\partial}{\partial \theta} [P_l^m(\cos \theta)] \vec{e}_\phi \right) V(r) \exp(im\phi), \quad (1a)$$

$$\begin{aligned} \vec{H}_{l,m} = & \left\{ \frac{l(l+1)}{r} V(r) P_l^{(m)}(\cos \theta) \vec{e}_r + \left(\frac{\partial}{\partial \theta} [P_l^{(m)}(\cos \theta)] \vec{e}_\theta \right. \right. \\ & \left. \left. + \frac{im}{\sin(\theta)} P_l^{(m)}(\cos \theta) \vec{e}_\phi \right) \frac{1}{r} \frac{\partial}{\partial r} [rV(r)] \right\} \exp(im\phi), \end{aligned} \quad (1b)$$

where $\vec{e}_r, \vec{e}_\theta, \vec{e}_\phi$ are unit vectors in the $\vec{r}, \vec{\theta}, \vec{\phi}$ directions, respectively, $P_l^{(m)}(\cos \theta)$ is an associated Legendre function, and $V(r) = Ah_l^{(1)}(kr) + Bh_l^{(2)}(kr)$, where $k = \sqrt{\epsilon} \omega / c$, $h_l^{(1)}(x)$ and $h_l^{(2)}(x)$ are spherical Hankel functions with constant coefficients A and B .

Similarly, for the TM eigenmodes,

$$\begin{aligned} \vec{H}_{l,m} = & \sqrt{\epsilon} k \left(\frac{m}{\sin \theta} P_l^{(m)}(\cos \theta) \vec{e}_\theta \right. \\ & \left. + i \frac{\partial}{\partial \theta} [P_l^{(m)}(\cos \theta)] \vec{e}_\phi \right) V(r) \exp(im\phi), \end{aligned} \quad (2a)$$

$$\begin{aligned} \vec{E}_{l,m} = & \left\{ \frac{l(l+1)}{r} V(r) P_l^{(m)}(\cos \theta) \vec{e}_r + \left(\frac{\partial}{\partial \theta} [P_l^{(m)}(\cos \theta)] \vec{e}_\theta \right. \right. \\ & \left. \left. + \frac{im}{\sin(\theta)} P_l^{(m)}(\cos \theta) \vec{e}_\phi \right) \frac{1}{r} \frac{\partial}{\partial r} [rV(r)] \right\} \exp(im\phi). \end{aligned} \quad (2b)$$

Note that the radial dependence of the tangential component of the electric field is given by $V(r) = Ah_l^{(1)}(kr) + Bh_l^{(2)}(kr)$ for the TE polarization, while this expression describes the tangential component of the magnetic field for TM polarization.

Now consider a sphere of radius r_0 made of material having a refractive index n_1 surrounded by a medium with refractive index n_2 . An electromagnetic field inside the sphere can be represented as the sum of incoming and outgoing spherical waves. However, the field at the center of the microcavity should be finite, which, in the case of an empty microcavity, requires that the incoming and the outgoing waves have equal amplitudes in the central core and the radial dependence of the field is described by a spherical Bessel function $j_l^{(1)}(x) = [h_l^{(1)}(x) + h_l^{(2)}(x)]/2$. Thus, the electromagnetic field of the eigenmodes is described by Eqs. (1) and (2) with $V(r) = j_l(kr)$. On the other hand, at the interface of the sphere and the surrounding medium, the amplitude of the ingoing wave must be equal to the product of the amplitude of the outgoing wave and the amplitude reflection coefficient R of that spherical wave from the boundary of the sphere. Hence, the equation for the optical eigenmodes of a spherical microcavity with radius r_0 can be represented in the form

$$R^{(\text{TE,TM})} h_l^{(1)}(kr_0) = h_l^{(2)}(kr_0). \quad (3)$$

Equation (3) defines the eigenfrequencies of both the TE and TM eigenmodes. We note here that in the case of the TE mode the reflection coefficient $R^{(\text{TE})}$ is defined as the ratio of the tangential component of electric fields for the ingoing and outgoing waves, while for the TM wave $R^{(\text{TM})}$ is the ratio of the tangential components of the magnetic fields.

The reflection coefficient⁷ for the TE polarization is given by

$$R^{(\text{TE})} = \frac{C_{l1}^{(1)} - C_{l2}^{(1)}}{C_{l2}^{(1)} - C_{l1}^{(2)}} \quad (4)$$

and for the TM wave by

$$R^{(\text{TM})} = \frac{-C_{l1}^{(1)}/\epsilon_1 + C_{l2}^{(1)}/\epsilon_2}{-C_{l2}^{(1)}/\epsilon_2 + C_{l1}^{(2)}/\epsilon_1}, \quad (5)$$

where $C_{ls}^{(1,2)} = -\frac{c}{\omega r} \frac{d}{dr} [r h_l^{(1,2)}(k_s r)] / h_l^{(1,2)}(k_s r)$, in which $k_s = \sqrt{\epsilon_s} \omega / c$ with $s=1$ or 2 and the whole expression is evaluated at $r=r_0$.

Substituting Eq. (4) into Eq. (3), one can write the equation for the eigenfrequencies of the TE modes in the form

$$\begin{aligned} h_l^{(1)}(k_2 r_0) [j_l(k_1 r_0) + k_1 r_0 j_l'(k_1 r_0)] - j_l(k_1 r_0) [h_l^{(1)}(k_2 r_0) \\ + k_2 r_0 h_l^{(1)'}(k_2 r_0)] = 0. \end{aligned} \quad (6)$$

Similarly, substituting Eq. (5) into Eq. (3), the equation for the eigenfrequencies of the TM modes has the form

$$\begin{aligned} \epsilon_2 h_l^{(1)}(k_2 r_0) [j_l(k_1 r_0) + k_1 r_0 j_l'(k_1 r_0)] - \epsilon_1 j_l(k_1 r_0) [h_l^{(1)}(k_2 r_0) \\ + k_2 r_0 h_l^{(1)'}(k_2 r_0)] = 0. \end{aligned} \quad (7)$$

Equations (6) and (7) can also be obtained by matching the tangential components of the electric and magnetic fields taken from Eqs. (1) and (2). In the case of large sphere radius the asymptotic expressions for the spherical Hankel functions, viz., $h_l^{(1,2)}(kr) \rightarrow \mp \frac{i}{kr} \exp(\pm i[kr - \frac{\pi l}{2}])$, can be used to obtain a simplified equation for the real part of the frequency of the eigenmode of the sphere,

$$\frac{2n_1 r_0 \omega^{(\text{TE,TM})}}{c} \approx \pi(2N + l) - \arg(R^{(\text{TE,TM})}). \quad (8)$$

For a gallium arsenide (GaAs) sphere in vacuum $\arg(R^{(\text{TE})}) \approx 0$ and $\arg(R^{(\text{TM})}) \approx \pi$, so that

$$n_1 r_0 \omega^{(\text{TE})} \approx \frac{\pi c(2N + l)}{2}, \quad (9a)$$

$$n_1 r_0 \omega^{(\text{TM})} \approx \frac{\pi c(2N + l + 1)}{2}. \quad (9b)$$

In the subsequent analysis, we will use the double index lN , where N is the radial quantum number in order to define the specific mode.

The minimum radius of the sphere at which a mode of frequency ω with a specific l exists (which will be referred to subsequently as the first mode TE/ l , TM/ l), can be estimated from Eq. (9a) for the TE polarization by putting $N=0$,

$$n_1 r_0^{(\text{TE})} \omega^{(\text{TE})} \approx \frac{\pi c l}{2}. \quad (10a)$$

For the TM polarization the corresponding result is

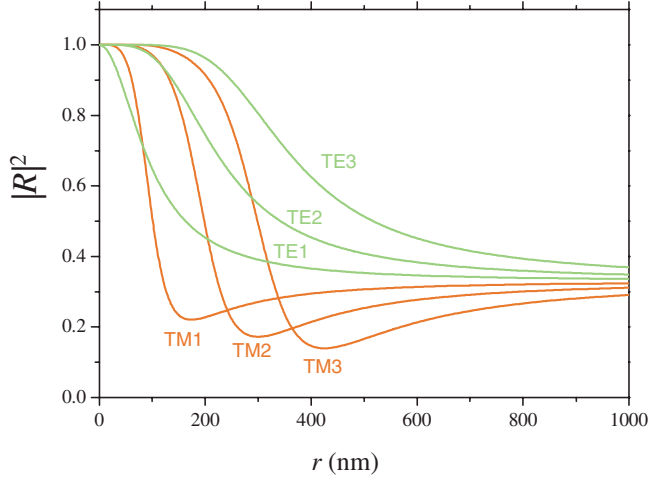


FIG. 1. (Color online) Power reflection coefficients of TE and TM outgoing spherical waves with $l=1, 2$, and 3 incident on a spherical interface of radius r . The refractive indices of the sphere and the surrounding medium are 3.7 (appropriate to GaAs) and 1.0 , respectively.

$$n_1 r_0^{(\text{TM})} \omega^{(\text{TM})} \approx \frac{\pi c(l+1)}{2}. \quad (10b)$$

However, for radial quantum number $N=0$, the radius of the sphere is comparable to the wavelength corresponding to the eigenmode energy, and the formulas in Eqs. (9) and (10) are not good approximations. Better approximations can be made by observing that if the refractive index of the sphere is larger than that of the outer medium, the electric field of the eigenmode should have an antinode at the boundary of the sphere. It follows from Eqs. (6) and (7) that $j_l(kr)$ should have a maximum at the boundary of the sphere for a TE mode, while $j'_l(kr)$ has a maximum for a TM mode. Now, according to a theorem of Siegel, the first root of $j_l(x)$ is confined between the values $\sqrt{(l+1/2)(l+5/2)}$ and $\sqrt{2(l+3/2)(l+7/2)}$ while the first root of $j'_l(x)$ is confined between the values $\sqrt{(l+1/2)(l+5/2)}$ and $\sqrt{2(l+1/2)(l+3/2)}$. Using these results it is possible to deduce an improved estimate of the minimum radius at which the first mode with a given l exists. For a TE mode, $r_0^{(\text{TE})}$ is given by

$$n_1 \omega^{(\text{TE})} r_0^{(\text{TE})} \approx 1.3c(l+1) \quad (11a)$$

whereas for the first TM mode,

$$n_1 \omega^{(\text{TM})} r_0^{(\text{TM})} \approx 1.3c(l+2). \quad (11b)$$

Equation (3) also allows an estimation of the decay rate γ of the amplitude of an optical eigenmode since it is given by the imaginary part of the corresponding eigenfrequency,

$$\gamma^{(\text{TE}, \text{TM})} = \frac{c}{2n_1 r_0^{(\text{TE}, \text{TM})}} \ln \left| \frac{1}{R^{(\text{TE}, \text{TM})}} \right|. \quad (12)$$

Representing the reflection coefficient $R^{(\text{TE})}$ as a Taylor series and substituting Eq. (11a) into Eq. (12) one can obtain an estimate for the decay of the first TE mode,

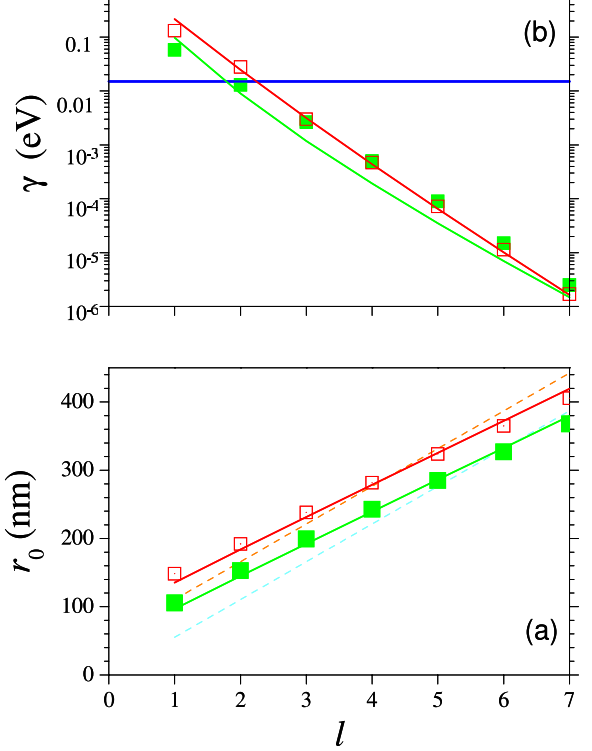


FIG. 2. (Color online) (a) Dependence on l of the minimum radius of a GaAs sphere at which a particular mode exists. The photon energy of the first mode with specific l and radial quantum number $N=0$ (TE/0, TM/0) is chosen to be 1.515 eV. Open (solid) symbols correspond to the value obtained for the TM (TE) polarization using Eqs. (6) and (7). The lines show the results obtained using the simplified Eq. (10) (dashed line) and Eq. (11) (solid line) for the eigenfrequencies of the cavity modes for the TM (upper/red) and TE (lower/green) polarizations. (b) Dependence on l of the radiative decay rate of the first mode ($N=0$, photon energy $=1.515$ eV). Open (solid line) symbols correspond to the value obtained for the TM (TE) polarization using Eqs. (6) and (7). The lines show the results obtained using the simplified Eq. (13) for the TM (upper/red) and TE (lower/green) polarizations. The horizontal solid line indicates the threshold between the weak-coupling and strong-coupling regimes.

$$\frac{\gamma}{\omega} = \frac{\alpha^{4l+1} 2^{l/2-5/2}}{\Gamma^4(l+3/2) n^{5l+1/2}}, \quad (13a)$$

where $\alpha=1.3(l+1)$ and $n=n_1/n_2$.

For the first TM mode the corresponding expression is

$$\frac{\gamma}{\omega} = \frac{\beta^{4l+1} 2^{l/2-5/2}}{\Gamma^4(l+3/2) n^{5l+1/2}}, \quad (13b)$$

where $\beta=1.3(l+2)$. When $3 < n < 4$, Eq. (13) can be simplified further to $\gamma/\omega \approx (n/3)^{-5l/2-1/2}$ for the first TE mode and $\gamma/\omega \approx (n/3)^{-5l/2-1/5}$ for the first TM mode.

The eigenfrequencies of the TE exciton-polariton modes of the spherical microcavity can be obtained from Eqs. (1a) and (1b) by including the excitonic contribution⁸ to the refractive index of the sphere. Our interest is in spheres that are much larger than the exciton radius and therefore a bulk model of the exciton and its dielectric response is appropri-

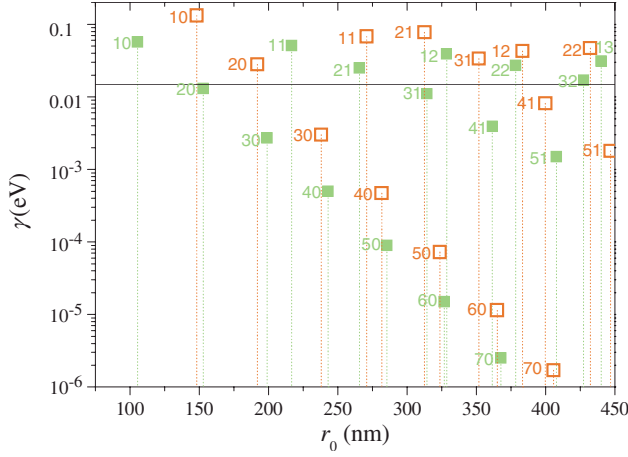


FIG. 3. (Color online) The radiative decay rate of the optical eigenmodes of a GaAs sphere as a function of the sphere radius for those modes with the real part of their eigenenergy equal to 1.515 eV for different values of l . The open (solid) squares correspond to the TM (TE) polarization, respectively. The index of the mode (lN) is shown to the left of each symbol. The horizontal line indicates the threshold between the weak-coupling and strong-coupling regimes.

ate. Accordingly, we take the refractive index n_1 of the sphere to be given by

$$n_1^2 = \epsilon_1 = \epsilon_b + \frac{\epsilon_b \omega_{LT}}{\omega_{ex} - \omega - i\Gamma}, \quad (14)$$

where ϵ_b is the background dielectric constant, ω_{ex} is the exciton resonance frequency, ω_{LT} is the bulk value of the longitudinal-transverse splitting, and Γ is the nonradiative decay rate of the exciton. In the numerical calculations for GaAs spheres, which are reported in Sec. III, we have taken $\epsilon_b = 13.69$, $\hbar\omega_{ex} = 1.515$ (eV), $\hbar\omega_{LT} = 0.08$ (meV), and $\hbar\Gamma = 1$ (meV). We have neglected the spatial dispersion of the excitons, which is weak in GaAs, and is even weaker in the wide band-gap semiconductors where the excitons are characterized by heavier effective masses.

To estimate analytically the value of the (Rabi) splitting Δ of the polariton modes, we consider how the exciton interaction affects an optical mode of the spherical cavity that would be at frequency ω_{ex} in the absence of excitonic effects, when the cavity would simply have a relative permittivity ϵ_b . For such a bare cavity mode, the cavity and mode parameters are related by Eq. (9) or Eq. (11), which can be rewritten in the form

$$\epsilon_b \omega_{ex}^2 r_0^{2(\text{TE, TM})} = A(l), \quad (15)$$

where $A(l)$ is the appropriate function of l . However, when excitonic effects are included, the relative permittivity of the cavity is $\epsilon_1 \approx \epsilon_b(1 + \frac{\omega_{LT}}{\omega_{ex} - \omega})$, if the nonradiative exciton decay is neglected, and the equation for the polariton eigenenergies is

$$\epsilon_b \left(1 + \frac{\omega_{LT}}{\omega_{ex} - \omega}\right) \omega^2 r_0^2 = A(l). \quad (16)$$

Combining Eqs. (15) and (16) yields

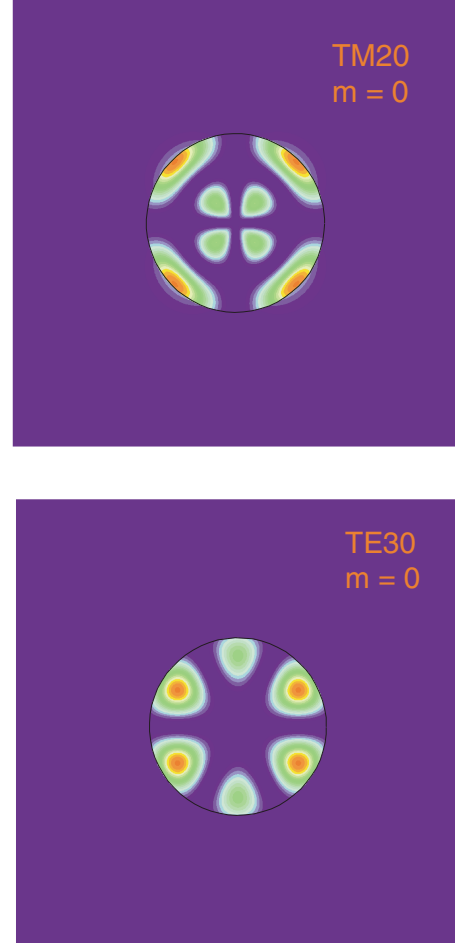


FIG. 4. (Color online) Cross section of the electric field squared for the TM20 mode (sphere radius $r_0 = 192$ nm and eigenenergy $= 1.515 - 0.028i$ eV) and the TE30 mode ($r_0 = 199$ nm and eigenenergy $= 1.515 - 0.0027i$ eV). The azimuthal number $m=0$ for both modes. Dark areas (blue) correspond to zero field and light areas (red) to high field.

$$\left(1 + \frac{\omega_{LT}}{\omega_{ex} - \omega}\right) \omega^2 = \omega_{ex}^2 \quad (17)$$

or

$$(\omega - \omega_{ex})(\omega + \omega_{ex}) - \frac{\omega^2 \omega_{LT}}{\omega - \omega_{ex}} = 0. \quad (18)$$

Assuming that $\omega - \omega_{ex} \ll \omega_{ex}$ we obtain

$$(\omega - \omega_{ex})^2 \approx \frac{\omega_{ex} \omega_{LT}}{2}. \quad (19)$$

Thus the splitting of polariton modes is

$$\Delta = \sqrt{2\omega_{ex}\omega_{LT}}. \quad (20)$$

This result is not exclusive to the case of spherical symmetry, but it is worth noting that the Rabi splitting for the sphere is generally larger than for planar microcavities with Bragg mirrors because the electric field of the cavity mode is mostly localized inside the sphere and thus its overlap inte-

gral with the exciton wave function of the corresponding symmetry approaches unity. On the other hand, in planar cavities the overlap integral is strongly reduced due to the penetration of the cavity mode into the dielectric Bragg mirrors.

III. RESULTS AND DISCUSSION

It follows from Eq. (12) that the radiative decay of the photon mode in a sphere depends on two factors, namely, the reflection coefficient of the spherical wave from the boundary of the sphere and the radius of the sphere. Minimization of γ can be achieved either by increasing the reflection coefficient R toward unity or by increasing the size of the sphere. However, increasing the size of the sphere leads to an increase in the density of photonic modes, which reduces the finesse of each individual mode.

Figure 1 shows for various outgoing spherical waves the dependence of the power reflection coefficient $|R|^2$ on the radius r of a spherical interface between GaAs with a refractive index $n_1=3.7$ (the incident medium) and vacuum ($n_2=1$). One can see that for $kr < l$ the reflection coefficient $|R|^2$ approaches unity with decreasing radius; for $kr > l$, $|R|^2$ asymptotically approaches the value $|(n_1-n_2)/(n_1+n_2)|^2$, which is the plane-wave limit. Note that the reflection coefficient always remains less than unity (strictly speaking, total internal reflection never takes place in the spherical geometry). Note also that for the TM modes there is a broad minimum in the dependence of $|R|^2$ on r , which is associated with the analog of the Brewster effect for spherical waves.⁷

According to Eqs. (10) and (11), the critical radius at which the first mode (TE₀, TM₀) of a GaAs sphere in vacuum comes into resonance with the bulk exciton energy, increases with increasing l , as illustrated in Fig. 2(a). Figure 2(b) shows the field amplitude decay rate γ corresponding to the photon modes, and this decreases nearly exponentially as l increases. It can be seen that only the TM modes with $l \geq 3$ and TE modes with $l \geq 2$ satisfy the strong-coupling condition.

Figure 3 shows the dependence on sphere radius r_0 of the decay rate of the mode with the real part of the eigenfrequency tuned to the exciton resonance in GaAs (1.515 eV). It can be seen that with increasing radius more and more modes (with radial quantum numbers $N=1, 2, 3$, etc.) appear. Equation (12) states that γ depends explicitly on the sphere radius r_0 and also implicitly on it through the reflection coefficient R [see Eqs. (4) and (5)]. It is instructive to consider increasing the sphere radius from an initial very small value. For a mode with specific l , the initial increase in sphere radius and the corresponding rapid decrease in reflection coefficient that is seen in Fig. 1 lead to an increase in γ . Further increase in sphere radius causes the reflection coefficient for a spherical wave at a spherical boundary to tend to the equivalent value for a planar surface, as shown in Fig. 1. At this point the sphere radius itself has more bearing on γ than the reflection coefficient does and, due to the inverse dependence of γ on r_0 , γ slowly decreases. On the other hand, in the limit of large radius, the density of modes becomes so large that even if many of the modes are formally strongly

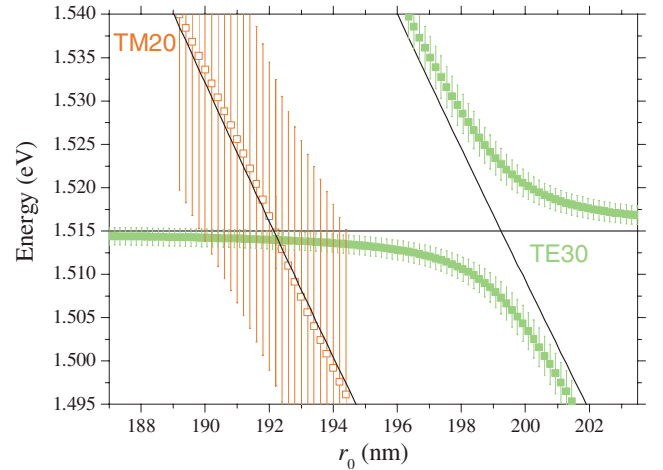


FIG. 5. (Color online) The real part of the photon energy of the first polariton modes of a GaAs sphere as a function of its radius. Within the interval of the radii considered only two bare optical modes exist: TM₂₀ and TE₃₀ (shown by solid lines). The vertical bars show the values of γ for the modes. The horizontal line shows the energy of the exciton resonance.

coupled with the exciton resonance, the finesse of the modes is so low that they are not suitable for polariton lasing. Figure 3 shows that one can always find a mode tuned to the specific frequency which possesses a substantial finesse and a sufficiently low decay rate but only for a value of l larger than unity. For example, if the radius of a GaAs sphere is just below 200 nm, the TE₃₀ mode has a decay rate below the threshold and is suitable for strong coupling, while the TM₂₀ mode is characterized by a decay rate just above the threshold.

Figure 4 shows the profile of the electric field for the TM₂₀ and the TE₃₀ modes for $m=0$. The TE₃₀ mode, having a decay rate $\gamma=3$ meV, is apparently almost perfectly localized within the sphere, while for the TM₂₀ mode with $\gamma=28$ meV, the tail of the field outside the sphere is visible. The difference in the penetration depth of the light field into the vacuum is responsible for the difference in their decay rates.

Figure 5 shows the dependence of the real parts of the eigenfrequencies of the TE₃₀ and TM₂₀ modes on sphere radius and the decay rates of these modes. The modes are not degenerate as predicted by the approximate formulae in Eqs. (9) and (11) but the difference in their energies is less than 5%. For the TM₂₀ mode, γ exceeds the Rabi splitting given by Eq. (18), which is characteristic of the weak-coupling regime. In contrast, for the TE₃₀ mode the decay rate is smaller than the Rabi splitting, so that the strong-coupling regime is realized, and this explains the anticrossing of the exciton and photon modes seen in the figure. The simple nature of semiconductor submicron spheres and the possibility of achieving strong coupling of photons and excitons in them suggest that they have significant promise for use in polariton lasers.

IV. CONCLUSIONS

For the optical modes of semiconductor spheres, we have considered the criteria for the simultaneous achievement of a

high finesse and a sufficiently high-quality factor to produce strong coupling with the exciton resonance in the semiconductor material. It is demonstrated numerically for the specific case of gallium arsenide spheres that the modes with smaller l are in the weak-coupling regime and the modes with larger l are in the strong-coupling regime. We have obtained the specific conditions required for the strong coupling of an exciton and an isolated photon mode which al-

lows the polariton dot to be considered as a promising candidate for use in a polariton laser.

ACKNOWLEDGMENTS

The work was supported in part by the EPSRC, the Royal Society, and the EU.

*On leave from the University of Southampton, Highfield, Southampton SO17 1BJ, United Kingdom.

¹S. Christopoulos, G. Baldassarri Höger von Högersthal, A. J. D. Grundy, P. G. Lagoudakis, A. V. Kavokin, J. J. Baumberg, G. Christmann, R. Butté, E. Feltin, J.-F. Carlin, and N. Grandjean, *Phys. Rev. Lett.* **98**, 126405 (2007).

²D. Bajoni, P. Senellart, E. Wertz, I. Sagnes, A. Miard, A. Lemaître, and J. Bloch, *Phys. Rev. Lett.* **100**, 047401 (2008).

³D. Bajoni, E. Semenova, A. Lemaître, S. Bouchoule, E. Wertz, P. Senellart, and J. Bloch, *Phys. Rev. B* **77**, 113303 (2008).

⁴A. A. Khalifa, A. P. D. Love, D. N. Krizhanovskii, M. S. Skolnick, and J. S. Roberts, *Appl. Phys. Lett.* **92**, 061107 (2008).

⁵S. I. Tsintzos, N. T. Pelekanos, G. Konstantinidis, Z. Hetzopoulos, and P. G. Savvidis, *Nature (London)* **453**, 372 (2008).

⁶See, e.g., A. V. Kavokin, J. J. Baumberg, G. Malpuech, and F. Laussy, *Microcavities* (Oxford University Press, Oxford, 2007).

⁷M. A. Kaliteevski, S. Brand, R. A. Abram, and V. V. Nikolaev, *J. Mod. Opt.* **48**, 1503 (2001).

⁸M. A. Kaliteevski, S. Brand, R. A. Abram, V. V. Nikolaev, M. V. Maximov, C. M. Sotomayor Torres, and A. V. Kavokin, *Phys. Rev. B* **64**, 115305 (2001).

⁹B. Gil and A. V. Kavokin, *Appl. Phys. Lett.* **81**, 748 (2002).

¹⁰M. A. Kaliteevski, S. Brand, R. A. Abram, A. Kavokin, and Le Si Dang, *Phys. Rev. B* **75**, 233309 (2007).

¹¹N. I. Nikolaev, A. Smith, and A. L. Ivanov, *J. Phys.: Condens. Matter* **16**, S3703 (2004).

¹²P. Bigenwald, V. V. Nikolaev, D. Solnyshkov, A. Kavokin, G. Malpuech, and B. Gil, *Phys. Rev. B* **70**, 205343 (2004).

¹³H. Ajiki and K. Cho, *Phys. Rev. B* **62**, 7402 (2000).

¹⁴H. Ajiki, T. Tsuji, K. Kawano, and K. Cho, *Phys. Rev. B* **66**, 245322 (2002).

¹⁵Despite the well-known fact that spherical light waves with $l = 0$ are forbidden because of the magnetic field divergence in the center of the sphere, the propagation of such waves through a multilayered spherical structure has been the subject of numerous computational studies, e.g., Er-Xuan Ping, *J. Appl. Phys.* **76**, 7188 (1994); *Electron. Lett.* **29**, 1838 (1993).

¹⁶R. Fuchs and K. L. Kliever, *J. Opt. Soc. Am.* **58**, 319 (1968).

¹⁷R. Ruppin, *Phys. Rev. B* **11**, 2871 (1975).

¹⁸D. S. Jones, *The Theory of Electromagnetism* (Pergamon, London, 1964), p. 483.

¹⁹W. K. H. Panofsky and M. Phillips, *Classical Electricity and Magnetism* (Addison-Wesley, London, 1962), p. 233.